SURE-BASED DUAL DOMAIN IMAGE DENOISING

Zhiya Xu[⋆,‡], *Tao Dai*[⋆,‡], *Li Niu*[†], *Jiawei Li*[⋆], *Qingtao Tang*[⋆], *Shu-Tao Xia*[⋆]

[⋆]Graduate School at Shenzhen, Tsinghua University, Shenzhen, Guangdong, China
[†] Electric and Computer Engineering department, Rice University, Houston, TX 77005, USA
Email: {zy-xu16, dait14}@mails.tsinghua.edu.cn

ABSTRACT

Recently developed Dual Domain Image Denoising (DDID) algorithm is a simple version of block-matching 3D filtering (BM3D) by combining bilateral filter and frequency-based method. DDID and its invariants have achieved competitive results compared with state-of-the-art methods. However, this kind of methods share a common drawback: there are a few parameters of the algorithms that are data- and noise-dependent, and difficult to tune. In this paper, we propose to use Stein's unbiased risk estimate (SURE) to measure the mean square error (MSE) of the DDID algorithm for restoration of an image contaminated with additive white Gaussian noise. We derive an explicit expression for SURE value to optimize parameters without access to the noise-free signal. Experimental results demonstrate the effectiveness of the proposed parameter selection in term of both quantitative and qualitative metrics.

Index Terms— Image denoising, Dual domain, Stein's unbiased risk estimate

1. INTRODUCTION

Image denoising is a fundamental problem in the filed of image processing and computer vision community [1, 2, 3, 4]. In general, image denoising methods can be classified as spatial domain methods, transform domain methods, or hybrid spatial-transform methods.

Spatial domain methods utilize various image prior knowledge of spatial structure, such as local correlation (*e.g.*, bilateral filter [5]), sparse representation (*e.g.*, group sparsity [6]), and nonlocal self-similarity (*e.g.*, non-local means filter [7]). This type of methods have tendency to remove low contrast details, and thus often over-smooth image contents. On the contrary, transform domain methods excel in preserving details like textures. This kind of methods can remove the noise effectively by thresholding coefficients in transform domain, which based on the assumption that images can be sparsely represented by orthonormal basis (*e.g.*, wavelets
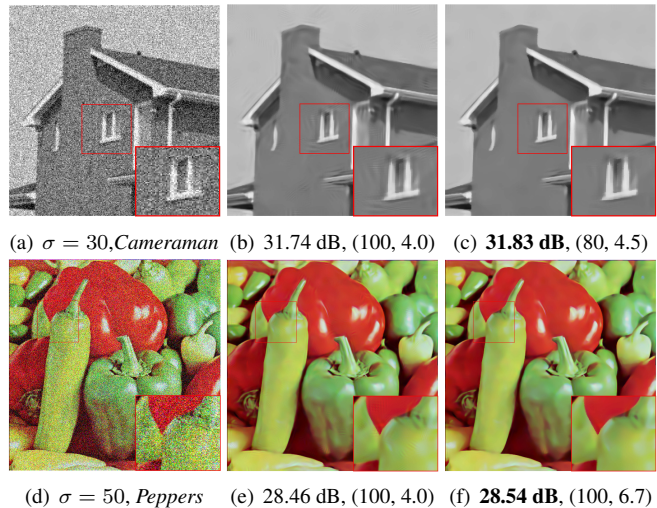
(a) $\sigma = 30$,*Cameraman* (b) 31.74 dB, (100, 4.0) (c) **31.83 dB**, (80, 4.5)

(d) $\sigma = 50$, *Peppers* (e) 28.46 dB, (100, 4.0) (f) **28.54 dB**, (100, 6.7)

Fig. 1. Denoised results of DDID with fixed parameters (the second column) and with optimal parameters selected by SURE optimization (the third column) for *Cameraman* and *Peppers*.

[8]). The transform based methods have the advantages of efficiency, but they often suffer from ringing artifacts near edges.

More advanced methods take advantage of both spatial and transform domain methods [9, 10, 11, 12]. Among them, block-matching and 3D (BM3D) [9] and BM3D-SAPCA [11] obtain remarkable results by combining non-local self-similarity and transform domain methods. Most recently, more efficient alternatives to the complex BM3D, like dual domain image denoising (DDID) [13] and its variants [14, 13, 15, 16], have been proposed. Such DDID based methods combine the simple bilateral filter and frequency-based methods in an iterative fashion, and provide denoising results generally superior to BM3D.

A remaining question of the original DDID algorithm is how to tune the parameters of the algorithm—the range parameter γ_r, and the wavelet shrinkage parameter γ_f, which are data-dependent and noise-dependent, thus resulting in their difficulty to tune. However, the original DDID adopt fixed parameters without considering image content and noise

levels. For example, as shown in Fig. 1, the denoised results of DDID show that it does not produce satisfying results (*e.g.*, ringing artifacts around edges) with the fixed parameters, while DDID with our SURE-based adaptive parameters obtains much better performance. Thus, the original DDID is sensitive to the choice of the parameters.

Contribution. To overcome this issue, in this paper, we propose to adopt the Stein's unbiased risk estimate (SURE) [17] as an unbiased estimator of the mean square error (MSE) of the DDID algorithm for denoising an image contaminated with additive white Gaussian noise. Our contributions can be summarized as: 1) We explore the role of the parameters γ_r and γ_f for the DIDD algorithm, and demonstrate that the optimal parameters are data-dependent and noise-dependent; 2) We derive an analytical expression for SURE that determines the optimal parameters by minimizing the SURE cost; 3) Experimental results not only confirm the optimality of the proposed parameter selection, but also reduce lots of artifacts comparing to the original DDID.

2. PRELIMINARIES

2.1. Stein's Unbiased Risk Estimate

Given an N-dimension noise-free image $\mathbf{x}$ contaminated with additive white Gaussian noise $\mathbf{n}$ with $n_i \sim \mathcal{N}(0, \sigma^2)$, where σ^2 is the variance of noise, and then the noisy image $\mathbf{y}$ is expressed as: $\mathbf{y} = \mathbf{x} + \mathbf{n}$. In image denoising task, mean square error (MSE) is computed between denoised image $\widehat{\mathbf{x}}$ and its reference image (clean image) to evaluate the performance of the denoised method. However, the reference image is often not available in practice. In [17], the principle of Stein's unbiased risk estimate (SURE) as an estimator for the MSE from the noisy image only was proposed. Specifically, SURE can be formulated as:

$$\text{SURE} = \frac{1}{N}||\mathbf{y} - \widehat{\mathbf{x}}||^2 - \sigma^2 + 2\sigma^2 \frac{\text{div}_{\mathbf{y}}\{\widehat{\mathbf{x}}\}}{N}, \qquad (1)$$

where $\text{div}_{\mathbf{y}}\{\widehat{\mathbf{x}}\}$ denotes the divergence of the denoising method with respect to the measurements

$$\text{div}_{\mathbf{y}}\{\widehat{\mathbf{x}}\} = \sum_{i \in \mathcal{I}} \frac{\partial \widehat{x_i}}{\partial y_i}. \qquad (2)$$

Note that using the SURE principle for optimal parameter selection has received much attention in different denoising methods for Gaussian distribution [18, 19, 20] and non-Gaussian distributions [21].

2.2. Dual Domain Image Denoising

DDID was first proposed by Knaus *et al.* in [12], including three nearly the same iterations. The basic idea of DDID is to split the images into high-contrast and low-contrast signals, which are processed by the bilateral filter and wavelet shrinkage method, respectively. The final denoised image $\widehat{\mathbf{x}}$ can

thus be the sum of two denoised layers: $\widehat{\mathbf{x}} = \widehat{\mathbf{x}}^l + \widehat{\mathbf{x}}^h$, where $\widehat{\mathbf{x}}^l$ and $\widehat{\mathbf{x}}^h$ denote the denoised results of low-contrast signals and high-contrast signals.

To filter a pixel centered at p from the noisy image $\mathbf{y}$, the first step of DDID extracts a patch $\mathcal{N}_p$ centered at p. The extracted patches are then processed by the bilateral filter, thus obtaining the denoised high-contrast value $\widehat{x}_p^h$:

$$\widehat{x}_p^h = \frac{\sum_{q \in \mathcal{N}_p} k_q y_q}{\sum_{q \in \mathcal{N}_p} k_q}, \qquad (3)$$

where the weight function k is

$$k_q = \exp\left(-\frac{|y_q - y_p|^2}{\gamma_r \sigma^2}\right) \exp\left(-\frac{||q - p||^2}{2\sigma_s^2}\right), \qquad (4)$$

and the parameters σ_s and γ_r control the decay of the exponential function; σ is the standard deviation of the noise. The first term in k identifies the pixels with similar structure to the center pixel, while the second term in k eliminates the periodization discontinuities with respect to a discrete Fourier transform (DFT).

After processing the high-contrast signals by the bilateral filter, we then obtain the low-contrast signals by subtracting the bilaterally filtered high-contrast values $\widehat{x}_p^h$, *i.e.*, $x_p^l = y_p - \widehat{x}_p^h$. Subsequently, wavelet shrinkage is used in the Fourier domain to remove the noise, thus yielding the denoised low-contrast value as follows:

$$\widehat{x}_p^l = \frac{1}{r^2} \sum_{f \in \mathcal{N}_F} K_f F_f, \qquad (5)$$

where $\mathcal{N}_F$ denotes the frequency domain (with size $r \times r$), $F = \mathscr{F}_p[k_q x_q^l]$ denotes the frequency coefficients in $\mathcal{N}_F$, and $\mathscr{F}_p[\cdot]$ means the DFT operation of the signals within $\mathcal{N}_p$; K_f is the corresponding the wavelet shrinkage factor: $K_f = \exp\left(-\frac{\gamma_f \sigma_f^2}{|F_f|^2}\right)$, where σ_f^2 represents the variance of the noisy frequency coefficients in $\mathcal{N}_F$, and γ_f is the wavelet shrinkage parameter. Thus, the final denoised value centered at p is the sum of the denoised low-contrast and high-contrast values:

$$\widehat{x}_p = \widehat{x}_p^l + \widehat{x}_p^h. \qquad (6)$$

The first step of DDID consists of the above processes repeated for each pixel of the image. Then the complete DDID algorithm repeats similar step three times with different parameters. For second and third step, the denoised result of the previous iteration is applied as a guide image, and please refer to [12, 15] to get more details about DDID.

3. SURE-BASED DDID

3.1. The analysis of the parameters in DDID

The above description shows that there exist two main parameters γ_r and γ_f in DDID. In this section, we will give some

analysis about the role of the parameters. As shown in Fig. 1, it can be seen that without proper parameter settings, DDID has a tendency to produce the annoying ringing artifacts in the denoised results. Thus, DDID is sensitive to the choice of γ_r and γ_f. To further see the effect of varying parameters, we plot the true MSE of DDID on various images and noise levels as a function of γ_r and γ_f in Fig. 2, which indicates that the optimal parameters are related to image contents and noise levels. These observations inspire us to propose a strategy to obtain the optimal parameters adaptively.

To obtain the optimal parameters, we use the SURE principle to monitor the MSE without access to noise-free images. The optimal parameters can be determined by minimizing the SURE cost. To compute the SURE, we derive an analytical expression, which will be shown in the following sections.

3.2. The derivation of SURE for DDID

As shown in Equ. (1), the divergence term in Equ. (2) plays a key role in the expression of SURE. From Equ. (6), we can see that the denoised value of DDID consists of two parts, *i.e.*, the denoised high-contrast value $\widehat{x}_p^h$ and low contrast value $\widehat{x}_p^l$. Thus, the divergence term can be computed as:

$$\frac{\partial \widehat{x}_p}{\partial y_p} = \frac{\partial \widehat{x}_p^h}{\partial y_p} + \frac{\partial \widehat{x}_p^l}{\partial y_p}, \qquad (7)$$

which is shown in the following two Propositions.

Proposition 1 *(Divergence of the high-contrast part $\widehat{x}_p^h$):*

The divergence of the high-contrast part $\widehat{x}_p^h$ is given by:

$$\frac{\partial \widehat{x}_p^h}{\partial y_p} = \frac{\sum_{q \in \mathcal{N}_p} k_q y_q^2}{\frac{1}{2}\gamma_r \sigma^2 W_p} + \frac{1}{W_p} - \frac{(\widehat{x}_p^h)^2}{\frac{1}{2}\gamma_r \sigma^2}, \qquad (8)$$

where $W_p = \sum_{q \in \mathcal{N}_p} k_q$.

Proposition 2 *(Divergence of the low-contrast part $\widehat{x}_p^l$):*

The second part $\widehat{x}_p^l$ is the denoised low-contrast signals by using wavelet shrinkage in the Fourier domain, as shown in Equ. (5). After some computation and simplification, the divergence of the low-contrast signals can be expressed as:

$$\frac{\partial \widehat{x}_p^l}{\partial y_p} =$$

$$\frac{1}{r^2} \sum_{f \in \mathcal{N}_F} K_f \left[\frac{\gamma_f}{|F_f|^2 \overline{F_f}} \left(\frac{4|F_f|^2}{\gamma_r} V_p + \sigma^2 A \sum_{q \in \mathcal{N}_p} k_q^2 \right) + \frac{\partial F_f}{\partial y_p} \right],$$
$$(9)$$

where $V_p = \sum_{q \in \mathcal{N}_p} k_q^2 (y_p - y_q)$, $A = \frac{\partial F_f}{\partial y_p} \overline{F_f} + F_f \frac{\overline{\partial F_f}}{\partial y_p}$,

$$\frac{\partial F_f}{\partial y_p} = \begin{cases} \mathscr{F}_p \left[k_p \left(\frac{2(y_q - y_p)(y_q - \widehat{x}_p^l)}{\gamma_r \sigma^2} - \frac{\partial \widehat{x}_p^l}{\partial y_p} \right) \right], & p \neq q \\ \mathscr{F}_p \left[1 - \frac{\partial \widehat{x}_p^l}{\partial y_p} \right], & p = q \end{cases}$$

where $\mathscr{F}_p[\cdot]$ means the DFT operation of the elements in $\mathcal{N}_p$.

Proposition 3 *(SURE for DDID):*

The parameter γ_f and γ_r are in Equ. (8) and Equ. (9). Then SURE-based optimization for the parameters can be formulated by substituting Equ. (7), (8), and (9) into Equ. (1)

$$\text{SURE}_{(\gamma_r, \gamma_f)} = \frac{||\mathbf{y} - \widehat{\mathbf{x}}||^2}{N} - \sigma^2 + \frac{2\sigma^2}{N} \sum_p^N \left(\frac{\partial \widehat{x}_p^h}{\partial y_p} + \frac{\partial \widehat{x}_p^l}{\partial y_p} \right).$$

Then the choice of the optimal parameters is equivalent to the following optimization problem as:

$$(\gamma_r, \gamma_f) = \arg\min_{\gamma_r, \gamma_f} \text{SURE}_{(\gamma_r, \gamma_f)}. \qquad (10)$$

4. EXPERIMENTAL RESULTS

4.1. Experimental setup

To test the performance of the proposed SURE-based DDID comprehensively, extensive experiments are performed on multiple test images from the standard image database. All the results are evaluated with PSNR and Structural Similarity index (SSIM) [22]. Each image is contaminated with AWGN with different amounts of noise, and we report the typical results ($\sigma = 30, 50, 70, 100$).
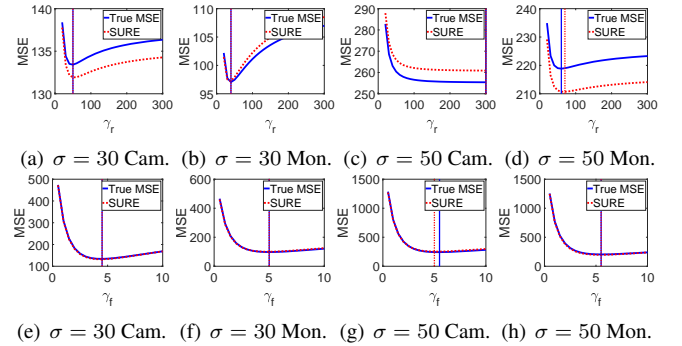

(a) $\sigma = 30$ Cam. (b) $\sigma = 30$ Mon. (c) $\sigma = 50$ Cam. (d) $\sigma = 50$ Mon.

(e) $\sigma = 30$ Cam. (f) $\sigma = 30$ Mon. (g) $\sigma = 50$ Cam. (h) $\sigma = 50$ Mon.

Fig. 2. Performance measures (true MSE (in blue), SURE (in red) for exact σ) as a function of the γ_r or γ_f. The optimal setting γ_r or γ_f for each measure is indicated by a vertical line in the same drawing style. The first and and second rows denote γ_r and γ_f with *Cameraman* (Cam.) and *Montage* (Mon.).

The first step of original DDID is parametrized by three parameters namely σ_s, γ_r, and γ_f, which are set to fixed constants in practice. In our experiments, we observe that the performance of DDID is not sensitive to the choice of σ_s, and thus we set the parameter σ_s to 7 as in DDID for a fair comparison. To test the influence of varying parameters γ_r and γ_f, we plot the true MSE of DDID on various images and noise levels as a function of the γ_r and γ_f. The parameter γ_r was ranged from 10 to 300 in steps of 10, and γ_f from 1 to 10

Table 1. Performance of DDID, and our method, and BM3D on various images and σ. The best results are highlighted in bold.

σ	Cameraman			House			Montage			Couple		
	DDID	Ours	BM3D	DDID	Ours	BM3D	DDID	Ours	BM3D	DDID	Ours	BM3D
30	28.58	**28.65(+0.07)**	28.64	31.74	31.83(+0.09)	**32.03**	31.33	**31.49(+0.17)**	31.37	28.61	28.65(+0.05)	**28.87**
	0.823	**0.832(+0.009)**	0.830	0.841	0.847(+0.006)	**0.849**	0.906	**0.916(+0.010)**	0.908	0.882	**0.893(+0.011)**	0.891
50	26.22	**26.26(+0.04)**	26.12	29.11	29.35(+0.24)	**29.64**	28.22	**28.41(+0.20)**	27.90	26.28	26.37(+0.090)	**26.46**
	0.757	0.764(+0.007)	**0.775**	0.798	**0.815(+0.017)**	0.813	0.854	**0.863(+0.009)**	0.857	0.804	**0.818(+0.014)**	0.815
70	24.57	**24.80(+0.23)**	24.61	27.23	27.63(+0.40)	**27.84**	26.14	**26.58(+0.44)**	25.92	24.76	24.79(+0.03)	**25.00**
	0.714	**0.736(+0.022)**	0.735	0.744	0.777(+0.033)	**0.782**	0.803	**0.824(+0.021)**	0.803	0.731	0.726(-0.005)	**0.749**
100	22.68	22.95(+0.27)	**23.07**	25.34	25.79(+0.44)	**25.99**	23.50	**23.95(+0.45)**	23.88	23.25	23.30(+0.05)	**23.51**
	0.650	**0.687(+0.037)**	**0.687**	0.692	0.737(+0.045)	**0.741**	0.733	**0.778(+0.045)**	0.744	0.640	0.634(-0.006)	**0.662**
σ	Peppers			Lena			Barbara			Man		
	DDID	Ours	BM3D	DDID	Ours	BM3D	DDID	Ours	BM3D	DDID	Ours	BM3D
30	29.35	**29.44(+0.08)**	29.28	**31.36**	31.27(-0.09)	31.26	**29.91**	29.83(-0.08)	29.81	28.73	28.78(+0.05)	**28.86**
	0.848	**0.855(+0.007)**	0.852	**0.919**	0.917(-0.002)	0.912	0.930	**0.931(+0.001)**	0.927	0.868	0.869(+0.001)	**0.875**
50	26.89	**26.96(+0.07)**	26.68	29.02	29.03(+0.01)	**29.05**	**27.40**	27.35(-0.05)	27.22	26.64	26.75(+0.11)	**26.81**
	0.789	0.792(+0.003)	**0.794**	0.870	**0.870(+0.000)**	0.867	0.883	**0.886(+0.003)**	0.872	0.788	**0.804(+0.016)**	0.801
70	25.07	**25.31(+0.24)**	25.06	27.39	27.52(+0.12)	**27.57**	25.70	**25.73(+0.03)**	25.47	25.32	25.48(+0.16)	**25.56**
	0.735	**0.754(+0.019)**	0.744	**0.829**	0.828(-0.001)	0.825	0.829	**0.832(+0.003)**	0.814	0.733	0.729(-0.004)	**0.747**
100	23.13	**23.45(+0.33)**	23.39	25.68	**25.97(+0.28)**	25.95	23.83	**23.93(+0.10)**	23.62	23.94	**24.22(+0.28)**	24.22
	0.678	**0.710(+0.032)**	0.683	0.770	**0.777(+0.007)**	0.768	0.756	**0.762(+0.006)**	0.738	0.661	0.663(+0.003)	**0.678**

in steps of 0.2. The optimal parameters for MSE and SURE for different images are shown in Fig. 2, from which we can have some observations: 1) The performance of DDID is sensitive the choice of the parameters; 2) The optimal parameters are related to image contents and noise levels. 3)The SURE approximates the MSE accurately and the optimal parameters obtained by SURE minimization is nearly the same as that by the true MSE.

4.2. Quantitative and qualitative analysis

As mentioned in section 2.2, a complete DDID algorithm is made up of three steps. In the second and third step of DDID, as most of the noise has already been removed, we set γ_r and γ_f to constant values empirically for simplicity. Specifically, we set $\{\gamma_r, \gamma_f\} = \{0.7, 0.4\}$ and $\{\gamma_r, \gamma_f\} = \{0.3, 0.7\}$ for the second and third step, respectively. In the case of color image, we filter in RGB space and our method is implemented in three channels independently.

The proposed method has been compared against the original DDID [12], and the advanced BM3D [9]. The parameters of these comparing methods are set in default values. PSNR and SSIM results are summarized in Table 1, from which we can see that our method obtains the best results in most cases. Specifically, the performance gain of our method over DDID increases with increasing noise levels, and the largest PSNR gain is up to 0.45 dB.

We also show the denoised results of different methods in Fig. 1 and Fig. 3, from which we can see that the denoised results of our method produce better visual quality than DDID and BM3D. For example, DDID and BM3D create noticeable artifacts in the denoised results (*e.g.,* the nose area of *Lena*), while our proposed method produces much more smooth results. Besides, the optimal parameters obtained by SURE minimization is nearly the same as that by the true MSE.
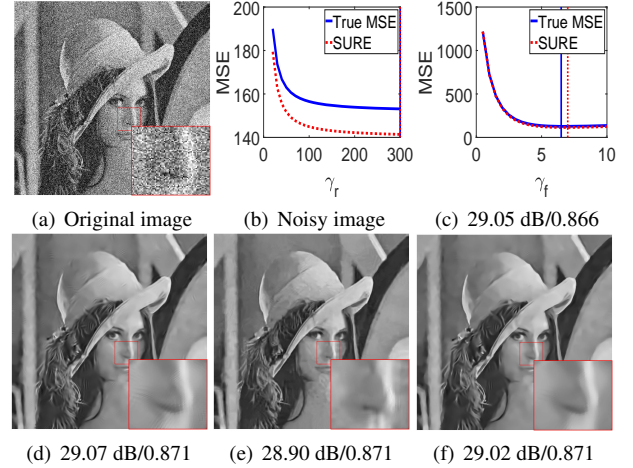

(a) Original image   (b) Noisy image   (c) 29.05 dB/0.866

(d) 29.07 dB/0.871   (e) 28.90 dB/0.871   (f) 29.02 dB/0.871

Fig. 3. Denoised results of the image *Lena* (at $\sigma = 50$) with (d) DDID, (e) BM3D, and (f) our method. (c) The optimal parameters by the true MSE and SURE cost. Zoom into PDF file for a detailed view.

5. CONCLUSIONS

We have proposed a technique for choosing the optimal parameters, which is dependent on image content and noise level, for the original DDID by minimizing the SURE cost, and have derived SURE expressions of DDID. We found the SURE is a useful metric to estimate and to tune the main parameters. Experiments verify that the obtained parameters based on the SURE principle is nearly the optimal parameters in the minimum MSE sense. Furthermore, the proposed method achieves better performance than the original DDID, and even obtains comparable results with other state-of-the-art denoising methods. Note that the parameter selection of our method can be easily extended to other DDID-based methods, like progressive image denoising (PID) [14].

6. REFERENCES

[1] Shao Ling, Yan Ruomei, Li Xuelong, and Liu Yan, "From heuristic optimization to dictionary learning: A review and comprehensive comparison of image denoising algorithms," *IEEE Transactions on Cybernetics*, vol. 44, no. 7, pp. 1001–1013, 2014.

[2] J. Xu, L. Zhang, W. Zuo, D. Zhang, and X. Feng, "Patch group based nonlocal self-similarity prior learning for image denoising," in *Computer Vision (ICCV), 2015 IEEE International Conference on*, Dec 2015, pp. 244–252.

[3] Antoni Buades, Bartomeu Coll, and Jean-Michel Morel, "Image denoising methods. a new nonlocal principle," *SIAM review*, vol. 52, no. 1, pp. 113–147, 2010.

[4] Zhiyuan Zha, Xin Liu, Ziheng Zhou, Xiaohua Huang, Jingang Shi, Zhenhong Shang, Lan Tang, Yechao Bai, Qiong Wang, and Xinggan Zhang, "Image denoising via group sparsity residual constraint," in *Acoustics, Speech and Signal Processing (ICASSP), 2017 IEEE International Conference on*. IEEE, 2017, pp. 1787–1791.

[5] Tao Dai, Weizhi Lu, Wei Wang, Jilei Wang, and Shu-Tao Xia, "Entropy-based bilateral filtering with a new range kernel," *Signal Processing*, vol. 137, pp. 223–234, 2017.

[6] Qiong Wang, Xinggan Zhang, Yu Wu, Lan Tang, and Zhiyuan Zha, "Nonconvex weighted l_p minimization based group sparse representation framework for image denoising," *IEEE Signal Processing Letters*, vol. 24, no. 11, pp. 1686–1690, 2017.

[7] Antoni Buades, Bartomeu Coll, and Jean-Michel Morel, "A review of image denoising algorithms, with a new one," *Multiscale Modeling & Simulation*, vol. 4, no. 2, pp. 490–530, 2005.

[8] S Grace Chang, Bin Yu, and Martin Vetterli, "Adaptive wavelet thresholding for image denoising and compression," *IEEE Transactions on Image Processing*, vol. 9, no. 9, pp. 1532–1546, 2000.

[9] K. Dabov, A. Foi, V. Katkovnik, and K. Egiazarian, "Image denoising by sparse 3-d transform-domain collaborative filtering," *IEEE Transactions on Image Processing*, vol. 16, no. 8, pp. 2080–2095, Aug 2007.

[10] Tao Dai, Chao-Bing Song, Ji-Ping Zhang, and Shu-Tao Xia, "Pmpa: A patch-based multiscale products algorithm for image denoising," in *Image Processing (ICIP), 2015 IEEE International Conference on*. IEEE, 2015, pp. 4406–4410.

[11] Kostadin Dabov, Alessandro Foi, Vladimir Katkovnik, and Karen Egiazarian, "Bm3d image denoising with shape-adaptive principal component analysis," in *SPARS'09-Signal Processing with Adaptive Sparse Structured Representations*, 2009.

[12] Claude Knaus and Matthias Zwicker, "Dual-domain image denoising.," in *Image Processing (ICIP), 2013 IEEE International Conference on*. IEEE, 2013, pp. 440–444.

[13] C Knaus and M Zwicker, "Dual-domain filtering," *SIAM Journal on Imaging Sciences*, vol. 8, no. 3, pp. 1396–1420, 2015.

[14] Claude Knaus and Matthias Zwicker, "Progressive image denoising," *IEEE Transactions on Image Processing*, vol. 23, no. 7, pp. 3114–3125, 2014.

[15] N. Pierazzo, M. Lebrun, M.E. Rais, J.M. Morel, and G. Facciolo, "Non-local dual image denoising," in *Image Processing (ICIP), 2014 IEEE International Conference on*. IEEE, Oct 2014, pp. 813–817.

[16] Tao Dai, Tang Qingtao Huang Kwok-Wai Zhang Yongbing Gu, Ke, and Shu-Tao Xia, "Foveated nonlocal dual denoising," in *Image Processing (ICIP), 2017 IEEE International Conference on*. IEEE, Sept 2017.

[17] Charles M. Stein, "Estimation of the mean of a multivariate normal distribution," *The Annals of Statistics*, vol. 9, no. 6, pp. pp. 1135–1151, 1981.

[18] Florian Luisier, Thierry Blu, and Michael Unser, "A new sure approach to image denoising: Interscale orthonormal wavelet thresholding," *IEEE Transactions on Image Processing*, vol. 16, no. 3, pp. 593–606, 2007.

[19] H. Kishan and C.S. Seelamantula, "Sure-fast bilateral filters," in *Acoustics, Speech and Signal Processing (ICASSP), 2012 IEEE International Conference on*, March 2012, pp. 1129–1132.

[20] Sathish Ramani, Thierry Blu, and Michael Unser, "Monte-carlo sure: A black-box optimization of regularization parameters for general denoising algorithms," *Image Processing, IEEE Transactions on*, vol. 17, no. 9, pp. 1540–1554, 2008.

[21] Yoann Le Montagner, Elsa D Angelini, and Jean-Christophe Olivo-Marin, "An unbiased risk estimator for image denoising in the presence of mixed poisson–gaussian noise," *IEEE Transactions on Image Processing*, vol. 23, no. 3, pp. 1255–1268, 2014.

[22] Zhou Wang, Alan Conrad Bovik, Hamid Rahim Sheikh, and Eero P Simoncelli, "Image quality assessment: from error visibility to structural similarity," *IEEE Transactions on Image Processing*, vol. 13, no. 4, pp. 600–612, 2004.